Flying Emplacement of an Underwater Glider

Dan Edwards, Nick Arnold, Stearns Heinzen, Chris Strem, and Trent Young
Vehicle Research Section
US Naval Research Laboratory
Washington, DC 20375

***Abstract* — An unmanned vehicle is envisioned for multi-modal operation, first as an aircraft, then as an underwater glider. The benefits of a "Flying Sea Glider" are for high-speed flying ingress above the water and then maneuvering in an area of interest as a low-speed, long-endurance underwater glider. This development builds on previous NRL research in multi-modal designs and bio-inspired propulsion systems, with a new emphasis on reducing power required in both air and underwater. Considerations for flying and underwater gliding vehicles are vastly different, despite the aero/hydrodynamic overlap. This paper explores design trades and analysis for a vehicle designed to operate in these two media. To explore the concept, NRL Test Sub 3 was developed and tested. The resulting vehicle demonstrated flight, splashdown, and gliding performance in one vehicle, validating the multi-modal flying and gliding design concept. Taken together with an analysis, the demonstration shows the viability of an unmanned "Flying Sea Glider" vehicle**

Keywords — air-water interface; unmanned air vehicle (UAV); unmanned underwater vehicle (UUV); air-deployed UAV; water landing; multi-modal operation; underwater glider.

I. Introduction

Autonomous underwater gliders are well-established sensing systems for long-range (trans-oceanic), deep (>1000m), and long-endurance (several months) oceanographic data collection. These craft move through the water using variable buoyancy to ascend or descend and have hydrodynamic lifting surfaces to transfer buoyancy-induced vertical motion into horizontal motion [1]. Speed through the water for a typical glider is on the order of 25cm/s, so pre-planning for operations of long distances is critical.

Several projects have investigated flying emplacement of an underwater vehicle [2-5] with the general goals of rapid ingress or repositioning above the water's surface. In those efforts, underwater propulsion is provided by traditional motor and propeller, flapping or undulating fins, or jets. A 2008 DARPA program named "Submersible Aircraft" [6] explored the feasibility of developing a single platform that is capable of both flying through the air and submerging below the water. This was explored in several papers [7-9]. Carrying humans presented challenges in designing for acceptable splashdown loads. Flying variants of existing underwater systems, such as wing-kits for sonobuoys [10] and torpedoes have been patented or built. For example, Lockheed Martin's HAAWC is a flying Mk-54 torpedo.

Previous work at NRL with bio-inspired fin propulsor mechanisms on a vehicle named WANDA [11] and a multi-modal vehicle named Flying-Swimmer (Flimmer) [12] explored flying submersible design with flapping propulsors. The original NRL Test Sub [13] was a flying submersible with conventional propeller for underwater propulsion. Both bio-inspired and conventional propulsion, though effective, require a significant amount of power, and the power source must be carried during the flying ingress. Even then, flight weight considerations limits battery size, restricting submerged operation to a relatively short duration after transition from flying. On the other hand, a Flying Sea Glider can operate underwater as a glider for long periods of time on relatively low power; flying emplacement mitigates the often undesirable slow ingress speeds typical of underwater gliders.

Underwater applications ranging from oceanography to virtual moorings to reconnaissance are all potentially enhanced

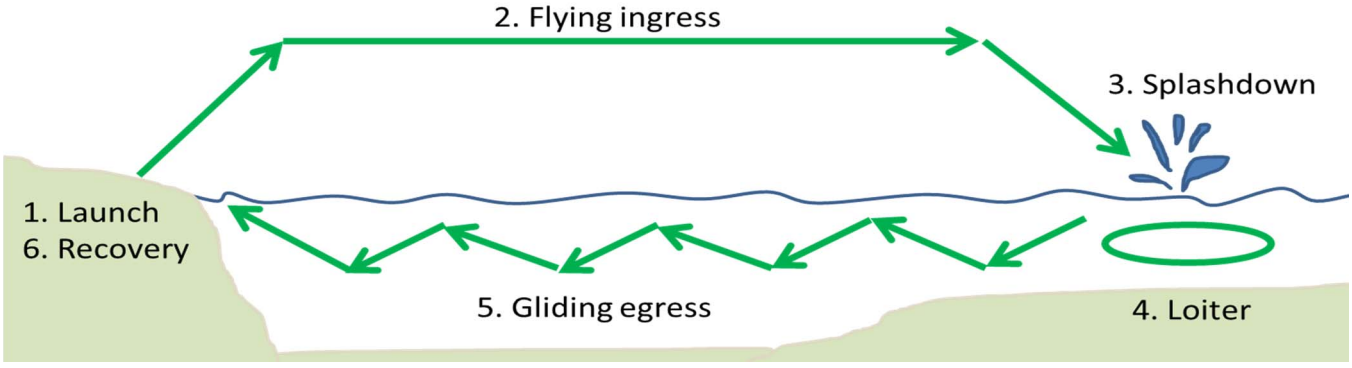

Fig. 1. Notional mission concept of operation for a Flying Sea Glider.

This work was funded by the Flying Sea Glider 6.2 NRL Base Program in Undersea Warfare.

using flying emplacement. However, the extra complexity from flying is likely only useful in certain cases, such as when rapid response is required or when traversing over high current areas that would otherwise be unreachable by a traditional underwater glider. Fig. 1 shows a notional concept of operation utilizing the technique of flying emplacement.

This paper presents the aero and hydrodynamic trade space overlap between flying and underwater gliding vehicles. The design and experimental results of the NRL Test Sub 3 vehicle are discussed, as an example of the multi-modal Flying Sea Glider concept. Finally, some conclusions are drawn about this configuration and prototype.

II. Multi-Modal Design Considerations

The aero and hydrodynamics for flying and underwater gliding are nearly identical with the exception of buoyancy terms added for underwater operation [1]. The operating conditions, however, are substantially different. While typical small-unmanned flying vehicles operate at velocities in the 10-60m/s range, sea gliding vehicles often cruise at less than 0.5m/s. The density of water is about three orders of magnitude greater than air, and the Reynolds numbers (ratio of inertial to viscous forces) while gliding are much lower than typical for flight.

Even more significant, the structural requirements and mass properties of the two configurations are vastly different. While flight vehicles are designed to be as light as possible and with a wing which can support several times the vehicle dry weight, underwater glider structural mass is dominated by the pressure vessel designed to resist pressure at depth, while lift forces are limited to some fraction of the net buoyancy force. Further, to operate as an underwater glider, the vehicle should be neutrally buoyant at a center-stroke buoyancy engine position. At that condition, the displaced water mass must equal the dry mass of the vehicle. This means the amount of displaced water will necessarily select the vehicle flying dry mass. Dry mass directly drives the power required to sustain level flight and the structural weight of the flying configuration, making it critical to reduce the trapped air volume as much as possible to keep flying mass (ergo power required) to a minimum.

The trade space between the two modes can be investigated by starting with the standard equations of flight. For an aircraft or glider in steady operation, lift is defined as:

$$L = 0.5\rho V^2 S C_L = W\cos\beta = mg\cos\beta \qquad (1)$$

Where ρ is the fluid density, V is velocity, S is wing reference area, C_L is coefficient of lift, β is glide path angle, and m is the dry mass of the vehicle for flight or the loaded mass (m_b) for underwater gliding.

For unaccelerated flight, thrust must equal drag (for gliding flight, thrust would be the component of weight along the flight path):

$$T = D = 0.5\rho V^2 S C_D = mg\sin(\beta) \qquad (2)$$

Where:

$$C_D = C_{Do} + C_{Di} = C_{Do} + \left(\frac{(mg)^2(\cos\beta)^2}{(0.5\rho V^2)^2 S^2}\right)\left(\frac{1}{\pi e AR}\right) \qquad (3)$$

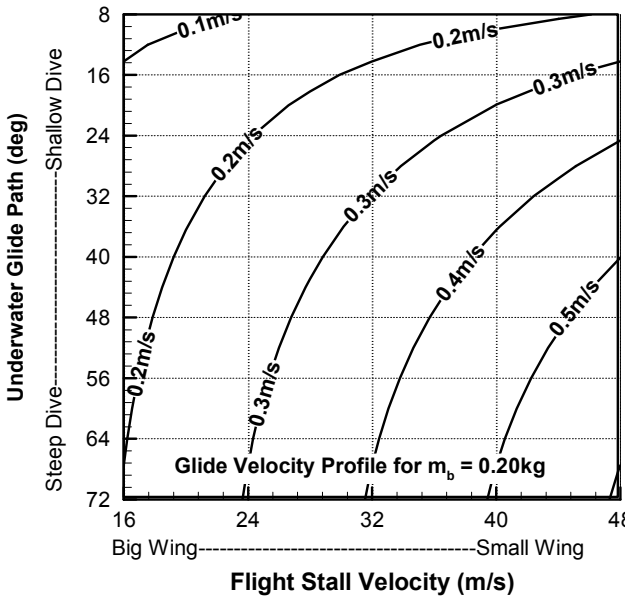

Fig. 2. Relationship between flying stall velocity (wing sizing), and underwater glide velocity at various glide path angles.

The drag coefficient in Eq. 3 is decomposed into two components. The first, C_{Do}, is the parasitic drag coefficient composed of friction forces and flow separation effects, and is typically estimated using empirical approaches, experimental testing, or computational analysis. The second, C_{Di}, is the induced drag, or drag due to lift, and is a measure of the efficiency of the wing at producing lift. The induced drag includes two additional terms related to wing efficiency, *e*, the Oswald efficiency factor, and the wing aspect ratio, *AR*.

Aircraft are typically constrained by a maximum lift coefficient which drives takeoff/launch velocities and/or wing sizing. After the wing sizing is defined, the amount of loaded mass available for buoyancy modification and the desired operating underwater glide path will determine the underwater gliding performance.

Examining a notional Flying Sea Glider configuration with a flying mass of 25kg and a loaded mass of ±0.2kg, it is apparent that the faster the flight stall velocity, and therefore the smaller the wing, the better the underwater performance. This is because, for a typical flying vehicle with a typical UAS launch velocity, the flight wing will generally be larger than a typical sea-gliding wing.

Figure 2 shows that to attain a 0.3m/s gliding velocity (in the typical range of operational gliders), the higher the stall velocity, the shallower an underwater glide angle can be achieved at the desired velocity, increasing transport efficiency by reducing the number of cycles required for distance traveled. This holds to a point, until the wing becomes small enough or the glide path angle becomes shallow enough that the required underwater C_L becomes too high to achieve at the low gliding Reynolds numbers (Fig. 3). Another result of the C_L variation with glide path angle is that induced drag, introduced in Eq. 3, quickly becomes inconsequential as glide path steepens and C_L becomes very small.

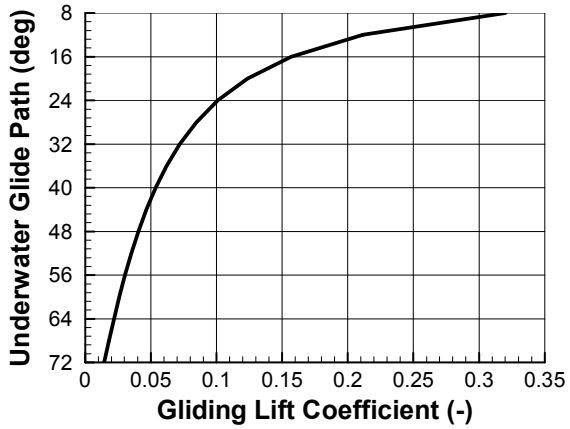

Fig. 3. Variation of lift coefficient with glide path angle showing the rapid rise in C_L at shallow angles.

A C_L of 1.0 is not uncommon in flying and is likely just fine for underwater also, so it is well within a designer's choice to select the underwater speed.

Further improvements in gliding speed can be achieved by increasing the amount of variable buoyancy, given that the hull hydrodynamics are fixed. Using air as the working fluid is lighter than using an oil-bladder mechanisms; increasing the variable volume is thus possible by stretching the mechanism stroke length and avoiding rapid mass growth.

III. Equipment

The design of the original Test Sub vehicle is outlined in Young [13]. Primarily, it was conceived as a conventional configuration with fuselage outer mold lines chosen for low drag underwater. All structure is flooded, with the exception of a small pressure vessel for housing the electronics and battery. Test Sub 3 is a gliding variant. The main vehicle specifications and calculated performance values are given in Table 1.

TABLE I. Test Sub 3 Specifications and Performance

	Value	Value
Dry mass	m	5kg
Variable mass	m_b	±75g
Wing span	b	1.0m
Wing area	S	0.084m^2
Aspect ratio	AR	10
Parasitic drag coeff.	C_{Do}	~0.04
Glide slope	Γ	35°
Lift to drag ratio	L/D	1.43
Glide velocity	V_{glide}	50 cm/s

The fuselage is a two-piece, hollow-molded fiberglass part built from female molds. The monocoque skin is the primary structural element and the wing, tail, and internal components mount to the skin. On the aft end of the fuselage, a firewall bulkhead allows bolting a small electric brushless motor for propulsion.

Both the wings and the tail surfaces are hollow-molded fiberglass skins. The wings each have a single plain flap control surface for roll axis control. The tail surfaces are full flying for ease of manufacture and actuation. Small holes drilled into the skin enable flooding.

Specific modifications of the original Test Sub for underwater gliding included removing several components: the brushless propulsion motor, electronic speed controller, air-bladder buoyancy control system and associated pumps, and separate battery pressure vessel.

One pressure vessel mounted inside the fuselage houses the electronics and battery. An inertial measurement unit, depth pressure sensor, microcontroller, and Wi-Fi module control the vehicle under the water. A single 2-cell 1.5Ah lithium polymer battery provides power.

For underwater gliding, a new piston-based buoyancy control system (Fig. 4) was developed and added. Two syringes were modified with waterproof (IP67) servos driving a lead screw to push the stock rubber gasket piston. The servo and piston assembly are on the flooded side. The buoyancy engine dry side is vented to the pressure vessel to use its air as a plenum. Together, the two buoyancy engines provide approximately ±75mL of variable volume. Mounting the buoyancy engines in the nose of the vehicle provided both buoyancy and pitch trim in the correct direction.

Another syringe with a ballast-filled piston and no air cavity was added for mass shifting control. The 200g piston can be moved approximately ±2cm. This addition proved to be ineffective for pitch control. Reasons for this are two-fold, resulting from the insufficient fraction of mass being shifted to move the center of gravity (CG), and the distance between the CG and center of buoyancy (CB) being relatively large.

Weight and balance was critical to the setup of the vehicle. First, the CG location was selected based on a desired stability margin for flight, placing the CG at approximately the wing quarter chord.

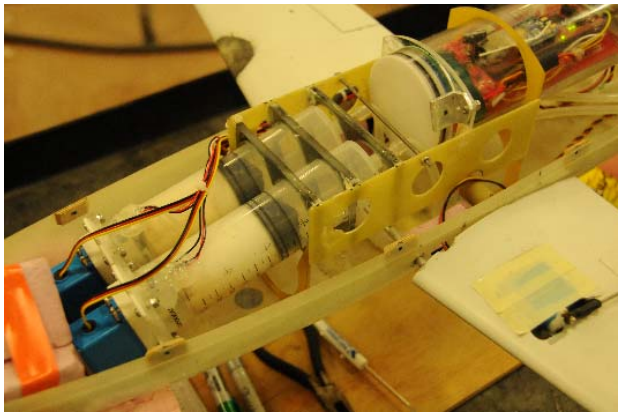

Fig. 4. Dual buoyancy engine mechanisms provide primary propulsive force in concert with the hydrodynamics.

The CG location choice also selected the CB location, as it must be at the same longitudinal location for level trim and below the CG for positive righting moment stability. To achieve a symmetric glide cycle, the vehicle CB was determined at the half-stroke position on the buoyancy engines.

Since Test Sub was highly sensitive to added weight and buoyancy, the internal components were temporarily mounted and the vehicle was trimmed for neutral buoyancy and level trim angle using a combination of foam and floatation ballast. The CG location was placed as low as possible and the CB location placed as high as possible within the hull to tailor pitch to buoyancy engine coupling to approximately 30 degrees at full buoyancy engine stroke.

A significant amount of weight was needed to achieve neutral buoyancy at the buoyancy engine half stroke, even though most of the internal vehicle volume was flooded; this highlights the need to minimize trapped air volume.

Meeting both the desired CG and CB location necessitated adding both ballast and floatation foam to the nose. Figure 4 shows the sealed plenum volume aft of the quarter chord, which drove to this solution.

IV. Flying Performance

The original Test Sub vehicle was designed without an airborne propulsion system and was thus dropped from a mothership aircraft. Typical testing consisted of a release from the mothership at approximately 300m above the water's surface and 15m/s airspeed. Test Sub fell away and increased airspeed to its cruise velocity of approximately 20-30m/s, and was manually controlled in a glide to a splashdown landing in the water. Fig. 5 illustrates the flight and splashdown phases of flight.

Three separate flights were performed with Test Sub [13], exploring the flight envelope and controllability of the configuration. The pilot reported positive control in all axes, noting the roll direction felt very sensitive, owing to the high roll inertia relative to the roll damping. Otherwise, the Test Sub configuration was well behaved. A glide speed of approximately 30m/s at a glide ratio of approximately 11 to 1 and a landing speed of approximately 20m/s was measured with a small GPS logger.

Two landing modes were explored: planing and plunge.

Shallower glideslopes with planing to bleed off kinetic energy slowly were anticipated to be the best entry method, owing to the slowest increase in deceleration drag. However, during testing, the lower vertical fin touched the water first and sheared off. Even with the lower vertical fin removed, the hull shape is not a planing design and would not have planed on the water surface.

In the other landing mode, a plunge landing with a steep pitch angle does not provide as slow of a deceleration force rise. However, it does load the structure in a relatively advantageous direction and provides a long deceleration time prior to the wing or tail surfaces touching the water.

(a)

(b)

Fig. 5. (a) Test Sub in flight after release from a mothership UAV, and (b) partly through the splashdown maneuver for the plunge landing.

A plunge landing with a pitch angle perpendicular to the water surface was tested. This maneuver resulted in excessive build-up of airspeed (approximately 45m/s), resulting in high impact loads.

The best landing method was a shallow approach and a pushover maneuver (instead of a flare) that put the nose into the water at approximately 45 degrees. This technique resulted in a reasonably slow entry speed and still allowed the nose to penetrate first to provide primary deceleration force prior to the wing and tail surfaces hitting water. No damage was noted after testing this landing technique.

Deceleration forces on splashdown were not measured. Photo evidence shows the 1m body length was fully submerged from a 20m/s entry speed, resulting in average deceleration forces of at most 20G's. Future efforts will explore using a parachute for reducing the landing loads.

V. Gliding Performance

Following flying ingress with a splashdown landing, the final performance objective of the Flying Sea Glider vehicle is to maneuver underwater using a buoyancy engine for propulsion.

Experiments to determine gliding performance were conducted in a 14m long by 7.5m wide by 1.5m deep tank filled with municipal water. Among other instrumentation, the tank is

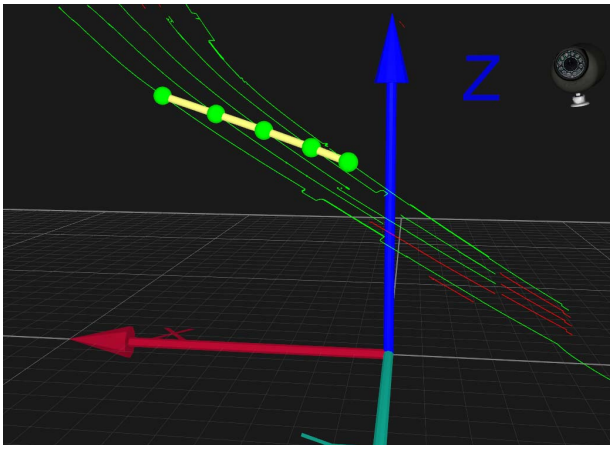

Fig. 6. Test Sub vehicle as viewed in underwater motion capture software showing markers along the longitudinal axis of the vehicle. The glide path is also shown in by the green lines.

outfitted with a 12-camera underwater motion capture system manufactured by Qualisys AB. When properly calibrated, this system allows for precise and accurate measurement of vehicle position and orientation through tracking of light-reflective markers positioned on the vehicle.

The Qualisys system was used to record the motion of the vehicle during a glide cycle, specifically with attention to the 2D longitudinal attitude and velocity vectors (Fig. 6). Seeking to understand and characterize the capabilities of Test Sub with the buoyancy engines driving its acceleration, data from several trials was collected after the vehicle had been trimmed in the water, shown (Table 2).

Measurements of Test Sub in the motion capture system showed glide speeds as fast as 12 cm/s and a max glide ratio of 2.5, resulting from a 4-degree angle of attack (AoA). Glide path angles varied between 21 to 40 degrees and AoA ranged between 4 to 30 degrees.

The large AoA resulted in stalled lift on the wings, reducing the L/D achieved. Additional pitch angle control would have helped reduce AoA and increased the L/D ratio. This is illustrated in Trial 6 where the AoA was 4 degrees and achieved the highest L/D at 2.5.

The indoor pool is shallow and it is unlikely that the measurements were operating in steady state. The dynamic interactions between the vehicle and pool's surface and bottom provide diversions from steady state behavior through surface tension and bringing Test Sub to rest prematurely. Also, the buoyancy engine run time and subsequent vehicle righting moment reaction and dampening all require more time to reach steady state than the 1.5m pool allows. A deeper tank with similar instrumentation is needed for better measurements.

Glide testing was moved to a 15m deep indoor tank, where Test Sub was unrestricted by depth to reach a steady state on ascent and descent. New issues relating to depth were uncovered. Despite the buoyancy engines successfully running to full positive, Test Sub did not rise to the surface from depth. We hypothesize that a combination of compressibility factors overrode the amount of buoyancy available. Small air bubbles trapped in tight locations, the permeability and compressibility of the floatation foam, and compression of air hoses between the buoyancy engine and plenum combined to overcome the positive buoyancy margin.

Experiments were also conducted outdoors in a local quarry with minimal instrumentation support (Fig. 7a). After some initial glides to 10m depth without an accompanying rise segment, some additional floatation foam was added to increase the buoyancy slightly. The vehicle was manually taken to 15m depth with the buoyancy engine in full rise and positive ascent rate was witnessed that verified the buoyancy margin was sufficient for compressibility effects.

An open-loop time, single dive cycle was set up for approximately 10m depth. A dive watch and timer were used to measure the depth profile (Fig. 7b). The buoyancy engine mechanism functioned as intended, providing roughly equal dive and rise rates. Glide distance was not measured, but a positive glide ratio in both descent and rise segments were observed. Calculated dive/rise rates of 4cm/s matches with the measurements in Table 2.

Elevator and ailerons were held streamlined during all glides. However, a more advanced controller could deflect the ailerons as flaperons to provide airfoil camber for improved lift capabilities and the elevator could be used to control angle of attack.

TABLE I. UNDERWATER GLIDING PERFORMANCE OF TEST SUB 3

Trial	L/D		Glideslope (deg)		V (cm/s)		V_h (cm/s)		V_z (cm/s)		AoA (deg)	
	Down	*Up*	*Down*	*Up*	*Down*	*Up*	*Down*	*Up*	*Down*	*Up*	*Down*	*Up*
1	1.48	1.47	34.0	34.3	10.4	6.32	9.14	3.29	5.00	5.40		
2	1.56	1.29	32.6	37.8	8.83	4.88	7.32	3.81	4.94	3.05		
3	2.08	1.15	25.6	41.0	7.57	6.10	6.71	4.42	3.51	4.21	16.6	29.0
4	1.45	1.54	34.7	33.0	7.92	7.84	6.71	6.61	4.21	4.21	25.8	24.2
5	1.56	1.29	32.6	37.8	8.83	4.88	7.32	3.81	4.94	3.05	16.5	28.9
6	2.50		21.8		9.06		7.62		4.91		3.97	
7	1.93		27.5		11.8		10.1		6.00		10.3	

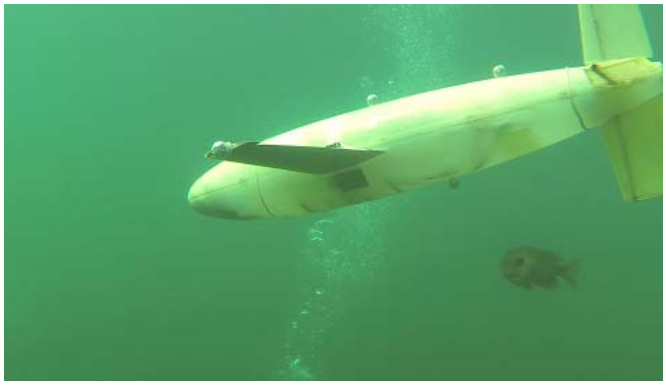

(a)

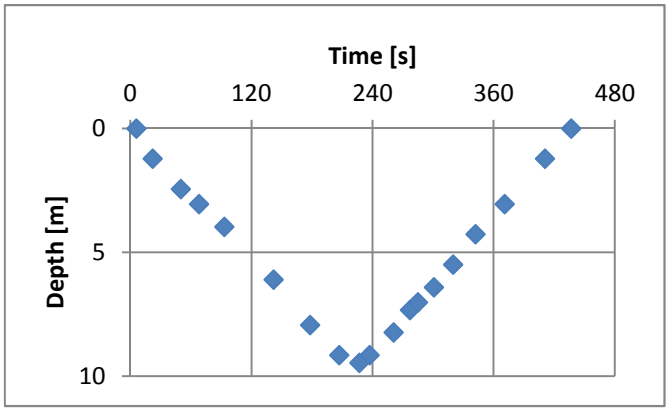

(b)

Fig. 7. (a) Test Sub operating in a quarry as an underwater glider using a buoyancy engine for propulsion, and (b) Dive profile measurements, buoyancy engine set for 10m depth, one cycle only.

The full-flying rudder deflected to approximately 30 degrees provided a 5m diameter turn. Turns were accomplished without any aileron deflection, as the natural stability from righting moment was sufficient to maintain wings-level attitude.

VI. Discussion and Conclusions

To explore the configuration design of a multi-modal flying and underwater gliding vehicle, a prototype design was fabricated and tested in both laboratory and real-world environments. The same outer mold lines operated as both an aircraft and an underwater glider. Measurements of vehicle performance validate the airborne flight segment is rapid (>30 m/s) when compared to the underwater gliding speed (12 cm/s). This supports the premise of using flying for ingress above the water surface and gliding below the surface for efficient underwater transport.

The flying segment is characterized primarily by the glide speed in the case of Test Sub, since there was no airborne propulsion motor. Glide speeds of 20-30 m/s were typical with a peak L/D of approximately 11. Control with ailerons and elevator was positive and enabled a pilot to guide the vehicle to a desired splashdown location. A shallow plunge splashdown landing was determined to have the least structural impacts on the vehicle.

Underwater, the inclusion of a ±75mL buoyancy engine and specific attention to the center of gravity relative to the center of buoyancy proved sufficient to achieve underwater glide motion of 12cm/s at 20deg glideslope, despite the large wing that was sized for flight. An ineffective mass-shift mechanism was installed and would have been better with longer throw, larger moving mass fraction, or shorter vertical righting moment. Measured glide speed is below expected performance as a result of transient dynamic effects from buoyancy transitions and surface/tank floor effects. The full-flying rudder was sufficient for steering control underwater and can be coupled with a more advanced autopilot in the future for closed-loop guidance.

Overall, the Test Sub experiments show there is significant overlap between flying and underwater gliding vehicles that is compatible for both media, and much was learned exploring the design considerations of multi-modal operations.

Lessons from the Test Sub design and experimentation are currently being used to develop a larger Flying Sea Glider toward a notional goal of 100nmi flying range, 200m dive depth, and two weeks of on-station gliding time.

References

[1] Jenkins, S., “Underwater Glider System Study”, Office of Naval Research, Technical Report 53, 6 May 2003.

[2] Goddard, R., Eastgate, J., “Submersible aircraft concept design study”, Naval Surface Warfare Center, Carderock Division, West Bethesda, MD, MSWCCD-2010/011, Aug 2010.

[3] T Aigeldinger, F Fish, “Hydroplaning by ducklings: overcoming limitations to swimming at the water surface”, Journal of Experimental Biology, Vol 198: pp 1567-1574, 1995.

[4] Maia, Marco M., Parth Soni, and Francisco J. Diez. "Demonstration of an aerial and submersible vehicle capable of flight and underwater navigation with seamless air-water transition." arXiv preprint arXiv:1507.01932 (2015).

[5] Xingbang Yang, Tianmiao Wang, Jianhong Liang, Guocai Yao, and Miao Liu. “Survey on the novel hybrid aquatic–aerial amphibious aircraft: Aquatic unmanned aerial vehicle (AquaUAV)”, Progress in Aerospace Sciences, Vol 74, Pp 131-151, April 2015.

[6] DARPA. Broad Agency Announcement: Submersible Aircraft. DARPA-BAA-09-06. 2008.

[7] Gilbert Crouse. "Conceptual Design of a Submersible Airplane", 48th AIAA Aerospace Sciences Meeting Including the New Horizons Forum and Aerospace Exposition, Aerospace Sciences Meetings, AIAA-2010-1012.

[8] Xingbang Yang, Tianmiao Wang, Jianhong Liang, Guocai Yao, and Wendi Zhao. "Submersible Unmanned Aerial Vehicle Concept Design Study", 2013 Aviation Technology, Integration, and Operations Conference, AIAA AVIATION Forum, (AIAA 2013-4422)

[9] Yao, Guocai, et al. "Submersible unmanned flying boat: Design and experiment." Robotics and Biomimetics (ROBIO), 2014 IEEE International Conference on. IEEE, 2014.

[10] Woodall, R. C., Garcia, F. A., “Standoff delivered sonobuoy”, US Patent 6082675A, 2000.

[11] R. Ramamurti, J.D. Geder, D.J. Edwards, and T.Z. Young, “Computational Studies for the Development of a Hybrid UAV/UUV”, proceedings of the AIAA Applied Aerodynamics Conference, AIAA-2015-2414, Dallas, TX, June 2015.